Optimal Detector Size in Multi–Slice CT

Marc Kachelrieß, Willi A. Kalender

Abstract— **Image data are noisy samples acquired at discrete positions. Signal processing explicitly or implicitly involves some kind of interpolation to match a desired point spread function, to match a certain spatial resolution or to match certain contrast detection criteria. By maximizing a resolution–, noise– and dose–dependent figure of merit $Q = Q(R, N, D)$ which is chosen as $Q^2 = 1/(RN^2D)$ for a one–dimensional detector and as $Q^2 = 1/(R^2N^2D)$ for a two–dimensional detector we determine the optimal detector size. In our case resolution R is the effective slice thickness S_{eff} that is given by the full width at half maximum of the slice sensitivity profile. In multi–slice CT reconstruction S_{eff} can be freely selected over a wide range of values starting from the collimated slice thickness S up to typically 10 mm. Our findings are that S_{eff} should be chosen at least 25% above the collimated slice thickness S. This choice increases dose usage by about 30% and corresponds to a dose reduction of 23% compared to a situation where $S_{\text{eff}} = S$.**

I. Introduction

It is common practice to push spatial resolution to the limit that is dictated by the size S of the detector elements. In most cases designers of CT hardware and image reconstruction software are afraid of losing spatial resolution. In multi–slice CT or cone–beam CT, for example, many efforts are taken to achieve an effective slice thickness — it is defined as the full width at half maximum (FWHM) of the slice sensitivity profile (SSP) — that equals the collimated slice width. There are numerous publications discussing issues of replacing slice–by–slice interpolation by some kind of conjugate ray interpolation just to avoid the 27% ($= 2 - \sqrt{3}$) increase of S_{eff} inherent to linear interpolating algorithms. Similarly, other authors are concerned that rebinning to parallel geometry may suffer from decreased transversal spatial resolution. They tend to use fan–beam backprojection algorithms that are computationally less efficient and theoretically more complex and less intuitive just to avoid an additional rebinning step.

Of course it is true that linear interpolation decreases spatial resolution. However, image noise is decreased, too! We will see that this decrease in image noise more than compensates for the decrease in spatial resolution and that one should simply use smaller detector elements instead of redesigning interpolation algorithms. For a given scanner this implies that reconstructions at maximum spatial resolution are far from optimal with respect to the tradeoff between noise, dose and spatial resolution [1].

II. Imaging System

We assume a rectangular presampling function of width S (collimated slice thickness) and area 1

$$s(z) = \text{II}^*_S(z) = \frac{1}{S}\,\text{II}\left(\frac{z}{S}\right);$$

Institute of Medical Physics (IMP), University of Erlangen–Nürnberg, Henkestraße 91, 91052 Erlangen. Corresponding author: Prof. Dr. Marc Kachelrieß, marc.kachelriess@imp.uni–erlangen.de.

a typical value for modern CT scanners is $S = 0.5$ mm.

Further, regard three representative interpolation algorithms of area 1 that allow a) to continue the discrete samples onto $\mathbb{R}$ and b) to balance between noise and spatial resolution:

$$\begin{aligned}
a_1(z) &= \text{II}^{**}_{w,w}(z) & \text{SSP}_1(z) &= \text{II}^{***}_{S,w,w}(z)\\
a_2(z) &= \text{II}^{**}_{S,w}(z) & \text{SSP}_2(z) &= \text{II}^{***}_{S,S,w}(z)\\
a_3(z) &= \frac{1}{\sqrt{\pi/3}\,w}e^{-3z^2/w^2} & \text{SSP}_3(z) &= \text{II}^*_S(z) * a_3(z).
\end{aligned}$$

The parameter w is a width parameter and will be used to adjust for optimal image quality. Note that for $w = S$ the first two algorithms correspond to simple linear interpolation (if we neglect the fact that the sampling distance between two detector rows slightly differs by the septa thickness δ from the width S of the presampling function). The third algorithm is a Gaussian interpolator that can be truncated after a few elements to remain finite–sized.

The algorithms a_i and their point spread functions $\text{SSP}_i = s * a_i$ are derived and plotted in reference [1]. The rectangle functions are recursively defined as $\text{II}^{**}_{a,b} = \text{II}^*_a * \text{II}^*_b$ and $\text{II}^{***}_{a,b,c} = \text{II}^{**}_{a,b} * \text{II}^*_c$.

Noise propagation through the algorithm $a(z)$ is characterized by the algorithm's noise factor

$$F^2 = \int dz\, a^2(z).$$

Given that the dose $\bar{D}$ captured by the detectors and contributing to the image is proportional to the product of patient dose D and of the geometric efficiency $S/(S+\delta)$ with δ being the thickness of the septa we find — after dropping constants of proportionality — that image noise is given by $N^2 = F^2/\bar{D} = F^2(S+\delta)/(SD)$.

The quantities F and N are analytically derived in reference [1] for the three algorithms.

III. Image Quality

Let

$$Q^2 = \frac{1}{S_{\text{eff}}N^2D} = \frac{1}{S_{\text{eff}}F^2}\frac{S}{S+\delta}$$

be the underlying measure of image quality that is to be optimized. Note that $Q_i = Q_i(\delta, S, S_{\text{eff}})$ for algorithm i. The spatial resolution S_{eff} is a function of w and vice versa; this relation depends on the algorithm type i as well. Further note that Q is a dimensionless quantity due to normalizing $a(x)$ and $s(x)$ to area 1.

We define the optimal detector size S for some desired spatial resolution S_{eff} as

$$S_i(\delta) = \underset{S}{\operatorname{argmax}}\, Q_i^2(\delta, S, S_{\text{eff}}).$$

IV. Results

The algorithms 1, 2, and 3 are shown in red, green, and blue color, respectively. To allow for reproduction on gray scale and even black and white printers the plot style is chosen to be solid, dotted, and dashed, respectively, for the three algorithms.

Figure 1 assumes that no septa are present. It demonstrates that it is of advantage to chose S_{eff} as large as possible with algorithms 1 and 3. Algorithm 2 is a trapezoidal interpolation that seeks for rather rectangular SSPs. This is either achieved for large or for small S_{eff} and only in–between, where $\text{SSP}_2(z)$ is bell–shaped, the curve exhibits a maximum.

Figures 2 corresponds to a far more realistic situation since septa are considered. It demonstrates how the detector size S influences image quality when the septum thickness is 0.1 and when a spatial resolution of $S_{\text{eff}} = 1$ is required. Obviously neither very small nor very large S are of advantage. The penalty for small detectors lies in the reduced dose usage due to the septa. Detectors as large as S_{eff} are of disadvantage since the resulting SSP is not bell–shaped and too much noise propagates into the image. Using the Gaussian algorithm and a slice thickness of about $0.5S_{\text{eff}}$ is optimal and increases Q_3^2 by a factor of 1.3 compared to the often used $S = S_{\text{eff}}$ combined with some triangular interpolation.

Optimal slice width S and achievable image quality Q as a function of the septum size δ is shown in the last figure. We can clearly see that $S \approx 0.5S_{\text{eff}}$ is a very good choice for moderate sized septa.

V. Discussion

Maximizing a dose–, noise– and resolution–dependent figure of merit Q shows that spatial resolution should be selected significantly below the theoretical limit given by the detector size. An increase of Q^2 by a factor of 1.3 was demonstrated for a typical CT situation. It corresponds to a dose reduction potential of 23% ($= 1 - 1/1.3$). Performing that optimization in both detector dimensions yields a dose reduction of 41% ($= 1 - 1/1.3^2$). Note that similar results are obtained when optimizing with respect to a contrast–to–noise at unit dose figure of merit [2]. This indicates that our findings are not specific to the figure of merit presented here but appear to apply for more general detection tasks.

Our recommendation in a nutshell: Reconstructions with a slice width S_{eff} that equals the collimated slice width S should be avoided. Choose $S_{\text{eff}} \geq 1.25S$ or higher.

References

[1] M. Kachelrieß and W. A. Kalender, "Presampling, algorithm factors and noise: Considerations for CT in particular and for medical imaging in general," *Med. Phys.*, vol. 32, pp. 1321–1334, May 2005.

[2] M. Kachelrieß and W. A. Kalender, "Optimizing detector size in x–ray imaging," *IEEE Medical Imaging Conference Program*, p. in press, Oct. 2005.

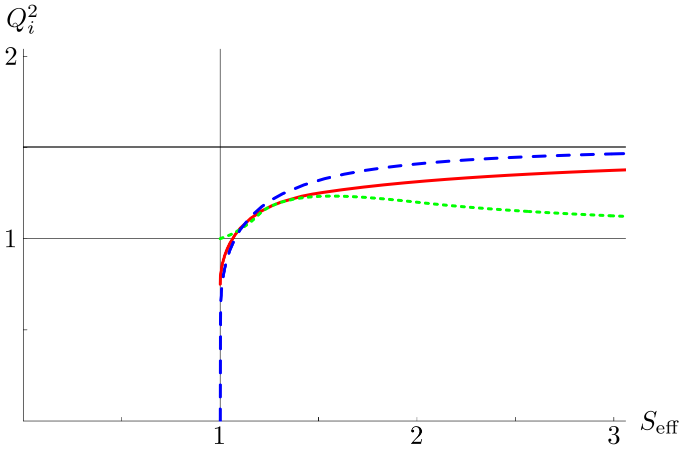

Fig. 1. Quality $Q_i^2(\delta, S, S_{\text{eff}})$ as a function of z–resolution S_{eff} for a fixed collimated slice thickness $S = 1$ and negligible septa $\delta = 0$. Horizontal lines show the asymptotic behaviour and the vertical line shows the lower limit of S_{eff} which is the width S of the aperture.

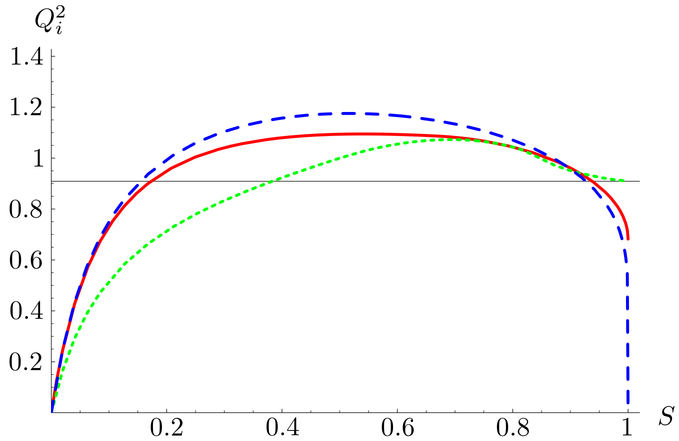

Fig. 2. Plot of $Q_i^2(\delta, S, S_{\text{eff}})$ as a function of S for $\delta = 1/10$ and $S_{\text{eff}} = 1$. The horizontal line is located at $1/(1+\delta) \approx 0.91$, the maximum of $Q_3^2(\delta, S, S_{\text{eff}})$ lies 30% higher. Obviously, about 30% quality (or dose efficiency) can be gained for this septa thickness by using detectors that are half of the size of the desired resolution.

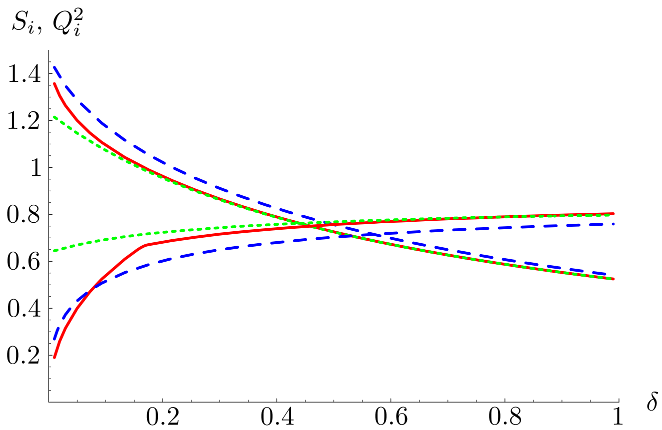

Fig. 3. To best achieve $S_{\text{eff}} = 1$ use these combinations. The plot shows optimum collimated slice thicknesses as a function of septa size δ (curves from lower left to upper right) and the corresponding Q_i^2–values (curves from upper left to lower right).